

# K<sup>+</sup>- and K<sup>-</sup>-production in heavy-ion collisions at SIS-energies

A. Förster for the KaoS-Collaboration:

I. Böttcher<sup>d</sup>, A. Förster<sup>a</sup>, E. Grosse<sup>f,g</sup>, P. Koczoń<sup>b</sup>,  
 B. Kohlmeyer<sup>d</sup>, S. Lang<sup>a</sup>, F. Laue<sup>b,\*</sup>, M. Menzel<sup>d</sup>,  
 L. Naumann<sup>f</sup>, H. Oeschler<sup>a</sup>, M. Płoskoń<sup>b</sup>,  
 F. Pühlhofer<sup>d</sup>, W. Scheinast<sup>f</sup>, A. Schmah<sup>a</sup>, T. Schuck<sup>c</sup>,  
 E. Schwab<sup>b</sup>, P. Senger<sup>b</sup>, Y. Shin<sup>c</sup>, H. Ströbele<sup>c</sup>,  
 C. Sturm<sup>a</sup>, F. Uhlig<sup>a</sup>, A. Wagner<sup>f</sup>, W. Waluś<sup>e</sup>

<sup>a</sup> Technische Universität Darmstadt, D-64289 Darmstadt, Germany

<sup>b</sup> Gesellschaft für Schwerionenforschung, D-64291 Darmstadt, Germany

<sup>c</sup> Johann Wolfgang Goethe Universität, D-60325 Frankfurt am Main, Germany

<sup>d</sup> Phillips Universität, D-35037 Marburg, Germany

<sup>e</sup> Uniwersytet Jagielloński, PL-30-059 Kraków, Poland

<sup>f</sup> Forschungszentrum Rossendorf, D-01314 Dresden, Germany

<sup>g</sup> Technische Universität Dresden, D-01062 Dresden, Germany

\* Present address: Brookhaven National Laboratory, USA

E-mail: a.foerster@gsi.de

**Abstract.** The production and the propagation of K<sup>+</sup>- and of K<sup>-</sup>-mesons in heavy-ion collisions at beam energies of 1 to 2 AGeV have systematically been investigated with the Kaon Spectrometer KaoS at the SIS at the GSI. The ratio of the K<sup>+</sup>-production excitation function for Au+Au and for C+C reactions increases with decreasing beam energy, which is expected for a soft nuclear equation-of-state. At 1.5 AGeV a comprehensive study of the K<sup>+</sup>- and of the K<sup>-</sup>-emission as a function of the size of the collision system, of the collision centrality, of the kaon energy, and of the polar emission angle has been performed. The K<sup>-</sup>/K<sup>+</sup> ratio is found to be nearly constant as a function of the collision centrality. The spectral slopes and the polar emission patterns are different for K<sup>-</sup> and for K<sup>+</sup>. These observations indicate that K<sup>+</sup>-mesons decouple earlier from the reaction zone than K<sup>-</sup>-mesons.

PACS numbers: 25.75.Dw

## 1. Introduction

Heavy-ion collisions provide the unique possibility to study baryonic matter well above saturation density. The conditions inside the dense reaction zone and the in-medium properties of hadrons can be explored by measuring the particles created in such collisions [1, 2]. In particular, the production of strange mesons at beam energies below or close to their respective threshold in binary nucleon-nucleon collisions ( $NN \rightarrow K^+ \Lambda N$

at  $E_{beam} = 1.6$  GeV,  $NN \rightarrow K^+K^-NN$  at  $E_{beam} = 2.5$  GeV) is well suited for these studies. The production at these energies requires multiple nucleon-nucleon collisions or secondary collisions like  $\pi N \rightarrow K^+Y$  ( $Y = \Lambda, \Sigma$ ) for the  $K^+$  or the strangeness exchange reaction  $\pi Y \rightarrow K^-N$  for the  $K^-$ . The propagation of  $K^+$ -mesons in nuclear matter is characterized by the absence of absorption (they contain an  $\bar{s}$ -quark and hence cannot be absorbed in hadronic matter consisting almost entirely of u- and d-quarks). In combination with the sensitivity to multi-step processes, which are more likely to occur at high particle densities, this absence of absorption makes them nearly undisturbed messengers carrying information on the hot and dense phase of the reaction. This allows to extract information on the nuclear equation-of-state [3, 4]. The  $K^-$  on the other hand can be reabsorbed via the inverse direction of the strangeness exchange reaction mentioned above. By analyzing observables sensitive to the reaction dynamics like energy distributions and angular distributions, both as a function of the size of the reaction system and of the collision centrality, the time dependence of the  $K^+$ - and of the  $K^-$ -emission can be investigated.

The experiments were performed with the Kaon Spectrometer (KaoS) at the heavy-ion synchrotron (SIS) at the GSI in Darmstadt [5]. The magnetic spectrometer has a large acceptance in solid angle and in momentum ( $\Omega \approx 30$  msr,  $p_{max}/p_{min} \approx 2$ ). The particle identification and the trigger are based on separate measurements of the momentum and of the time-of-flight. The trigger suppresses pions and protons by factors of  $10^2$  and of  $10^3$ , respectively. The background due to spurious tracks and pile-up is removed by a trajectory reconstruction based on three large-area multi-wire proportional counters. The short distance of 5 - 6.5 m from the target to the focal plane minimizes the number of kaon-decays in flight. The loss of kaons by decay is accounted for by Monte Carlo simulations using the GEANT code. Three different collision systems have been investigated (Au+Au, Ni+Ni, and C+C) at incident beam energies ranging from 0.6 AGeV to 2.0 AGeV. Results have been published in [6, 7, 8, 9, 10, 11, 3, 12] and will in part be presented in this contribution.

Section 2 briefly summarizes the results on the excitation function of the  $K^+$ -production and the conclusions that can be drawn on the nuclear equation-of-state. In section 3 a detailed analysis of dynamical observables for the reaction systems Au+Au and Ni+Ni at an incident beam energy of 1.5 AGeV is presented, followed by conclusions on the time dependence of the emission of  $K^+$ - and of  $K^-$ -mesons in section 4.

## **2. $K^+$ -production as a probe for the nuclear equation-of-state**

Early transport calculations predicted that the  $K^+$ -yield in Au+Au collisions at beam energies below the production threshold in nucleon-nucleon collisions would be enhanced by a factor of about 2 if a soft rather than a hard equation-of-state is assumed [1, 13]. Recent calculations take into account modifications of the kaon properties within the dense nuclear medium. The assumed repulsive  $K^+N$ -potential depends nearly (or less than) linearly on the baryonic density [14] and thus reduces the  $K^+$ -yield accordingly. On

the other hand, at subthreshold beam energies the K<sup>+</sup>-mesons are created in secondary collisions involving two or more particles and hence their production depends at least quadratically on the density. To disentangle these two competing effects we have studied the K<sup>+</sup>-production in a light (C+C) and in a heavy collision system (Au+Au) at different beam energies near threshold. The maximum baryonic density reached in Au+Au reactions is significantly higher than in C+C reactions. Moreover, the maximum baryonic density reached in Au+Au reactions depends strongly on the compression modulus of nuclear matter  $\kappa$  [15, 13] whereas in C+C collisions this dependence is rather weak [4]. Hence, the ratio of the K<sup>+</sup>-multiplicity per nucleon  $M/A$  in Au+Au to the one in C+C is expected to be sensitive to the compression modulus  $\kappa$  while providing the advantage that uncertainties within the experimental data (beam normalization etc.) and within the transport model calculations (elementary cross sections etc.) are partly cancelled.

Figure 1 shows a comparison of the ratio  $(M/A)_{\text{Au+Au}}/(M/A)_{\text{C+C}}$  for K<sup>+</sup> with the predictions of RQMD transport model calculations [4]. The calculations were performed with two values for the compression modulus:  $\kappa = 200$  MeV (solid line) and  $\kappa = 380$  MeV (dashed line) corresponding to a “soft” or “hard” nuclear equation-of-state, respectively. The RQMD transport model takes into account a repulsive K<sup>+</sup>N-potential and uses momentum-dependent Skyrme forces to determine the compressional energy per nucleon (i.e. the energy stored in the compression) as a function of the baryon density. The comparison demonstrates clearly that only the calculation based on a soft nuclear equation-of-state reproduces the trend of the experimental data. A similar result is obtained using the transport code IQMD [16].

### 3. K<sup>+</sup>- and K<sup>-</sup>-production at 1.5 AGeV

In this section detailed results of experiments on the production and on the propagation of K<sup>+</sup>- and of K<sup>-</sup>-mesons in Ni+Ni and in Au+Au collisions at a beam energy of 1.5 AGeV are presented. This is the lowest beam energy where K<sup>-</sup> have been observed so far in collisions between heavy nuclei. The spectral and the angular distributions of strange mesons as a function of the collision centrality have been measured and significant differences between K<sup>+</sup> and K<sup>-</sup> have been found [12].

Due to the energy loss in the Au-target (thickness 0.5 mm) the average energy of the Au-beam is 1.48 AGeV. The energy loss of the Ni-ions in the Ni-target is negligible. A high-statistics sample of K-mesons was recorded at a polar angle of  $\theta_{lab} = 40^\circ$ . Data from Au+Au collisions were also taken at  $\theta_{lab} = 32^\circ, 48^\circ, 60^\circ,$  and  $72^\circ$  with lower statistics. The laboratory momenta of the K-mesons range from 260 to 1100 MeV. Figure 2 shows the acceptance covered by these measurements as a function of the rapidity normalized to beam rapidity  $y/y_{beam}$  and of the transverse momentum  $p_\perp$ .

The centrality of the collision was derived from the multiplicity of charged particles measured in the interval  $12^\circ < \theta_{lab} < 48^\circ$  by a hodoscope consisting of 84 plastic-scintillator modules. In order to study the centrality dependence the data measured

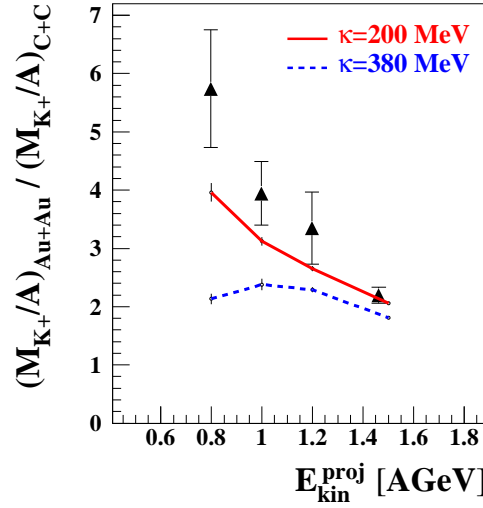


**Figure 1.** The ratio of the  $K^+$ -multiplicity per nucleon  $M/A$  in Au+Au to the one in C+C reactions as a function of the beam energy for inclusive reactions. The data are compared to the results of RQMD transport model calculations [4]. The calculations were performed with two different values for the compression modulus:  $\kappa = 200$  MeV (a “soft” equation-of-state), denoted by the solid line, and  $\kappa = 380$  MeV (a “hard” EoS), indicated by the dashed line.

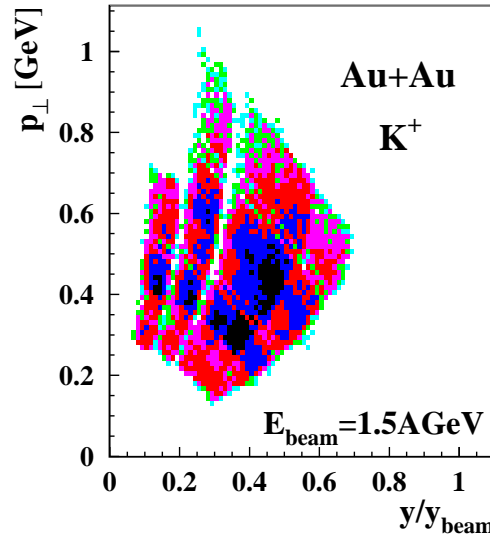


**Figure 2.** Transverse momentum  $p_{\perp}$  as a function of the rapidity  $y/y_{beam}$  for  $K^+$ . The different bands correspond to different spectrometer angles in the laboratory  $\theta_{lab}$ .

close to midrapidity ( $\theta_{lab} = 40^\circ$ ) were grouped into five centrality bins both for Ni+Ni and for Au+Au collisions. The most central collisions correspond to 5% of the total reaction cross-section  $\sigma_R$ , the subsequent centrality bins correspond to 15%, 15% and 25% of  $\sigma_R$ . The most peripheral collisions correspond to 40% of  $\sigma_R$ . The total reaction

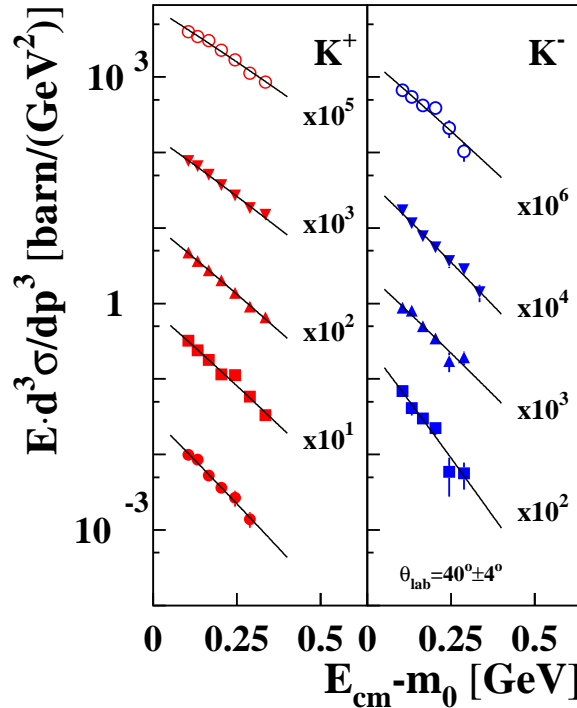


**Figure 3.** Invariant cross sections for  $K^+$  and for  $K^-$  in Au+Au collisions at  $E_{beam} = 1.5$  AGeV for the different centrality bins. The open circles depict the most central data, the other bins are shown from the top to the bottom of the figure with decreasing centrality. Due to low statistics the most peripheral bin is not shown for  $K^-$ .

cross-section was derived from a measurement with a minimum bias trigger and was found to be  $\sigma_R = 6.0 \pm 0.5$  barn for Au+Au and  $\sigma_R = 2.9 \pm 0.3$  barn for Ni+Ni collisions. The corresponding mean number of participating nucleons for each centrality bin  $\langle A_{part} \rangle$  was calculated from the measured reaction cross-section fraction for this bin using a geometrical model assuming spherical nuclei.

Figure 3 shows the production cross sections for  $K^+$ - and for  $K^-$ -mesons measured close to midrapidity as a function of the kinetic energy in the center-of-momentum system for the five centrality bins in Au+Au collisions. The uppermost spectra correspond to the most central reactions, the subsequent bins are shown from the top to the bottom of the figure with decreasing centrality. The error bars represent the statistical uncertainties of the kaon and the background events. An overall systematic error of 10% due to efficiency corrections and beam normalization has to be added. The solid lines represent the Boltzmann function  $d^3\sigma/dp^3 = C \cdot E \cdot \exp(-E/T)$  fitted to the data.  $C$  is a normalization constant and the exponential function describes the energy distribution with  $T$  being the inverse slope parameter.

The spectra presented in figure 3 exhibit a distinct difference between  $K^-$  and  $K^+$ : The slopes of the  $K^-$ -spectra are steeper than those of the  $K^+$ -spectra. The inverse

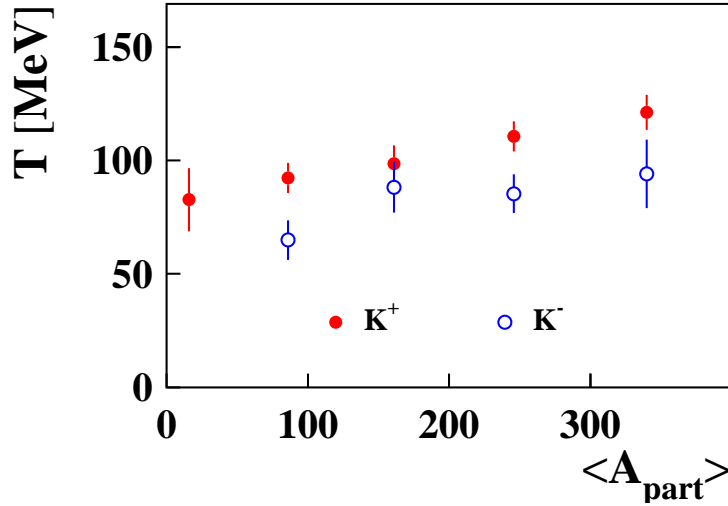


**Figure 4.** Inverse slope parameters  $T$  as a function of the number of participating nucleons  $\langle A_{part} \rangle$  for  $K^+$  (full symbols) and  $K^-$  (open symbols) in Au+Au collisions at 1.5 AGeV measured at  $\theta_{lab} = 40^\circ$ .

slope parameters  $T$  as a function of the mean number of participating nucleons  $\langle A_{part} \rangle$  for each centrality bin are displayed in figure 4.  $T$  increases with increasing centrality and is found to be significantly lower for  $K^-$  than for  $K^+$ , even for the most central collisions.

The multiplicities of  $K^+$ - and of  $K^-$ -mesons in Ni+Ni as well as in Au+Au collisions at 1.5 AGeV differ by about a factor of 50. The inclusive kaon multiplicity is defined for each centrality bin as  $M = \sigma_K / (f \cdot \sigma_R)$  with  $\sigma_K$  being the kaon production cross section and  $(f \cdot \sigma_r)$  being the fraction of the reaction cross-section for the particular event class. Figure 5 presents the multiplicity per number of participating nucleons  $M / \langle A_{part} \rangle$  as a function of  $\langle A_{part} \rangle$  for  $K^+$  (upper panel) and for  $K^-$  (middle panel). Both, for  $K^+$ - and for  $K^-$ -mesons the multiplicities exhibit a similar rise with  $\langle A_{part} \rangle$ . Moreover,  $M / \langle A_{part} \rangle$  is found to be almost identical in Ni+Ni and in Au+Au collisions. The resulting  $K^- / K^+$  ratio is about 0.02 below  $\langle A_{part} \rangle = 100$  and decreases slightly to about 0.015 for the most central collisions (lower panel).

Another observable sensitive to the production mechanism is the polar angle emission pattern. The deviation from isotropy of the  $K^+$ - and of the  $K^-$ -emission can be studied using the ratio  $\sigma_{inv}(E_{cm}, \theta_{cm}) / \sigma_{inv}(E_{cm}, 90^\circ)$  as a function of  $\cos(\theta_{cm})$ . Here,  $\sigma_{inv}(E_{cm}, \theta_{cm})$  is the invariant kaon production cross-section measured at the polar angle  $\theta_{cm}$  in the center-of-momentum frame and  $\sigma_{inv}(E_{cm}, 90^\circ)$  is the one measured at  $\theta_{cm} = 90^\circ$ . Due to limited statistics we considered only Au+Au collisions grouped into two centrality bins: near-central (impact parameter  $b < 6$  fm) and non-central collisions ( $b > 6$  fm). Figure 6 displays the anisotropy ratio for  $K^+$  (upper panels) and for  $K^-$  (lower panels), both for near-central (right) and for non-central collisions (left). For an

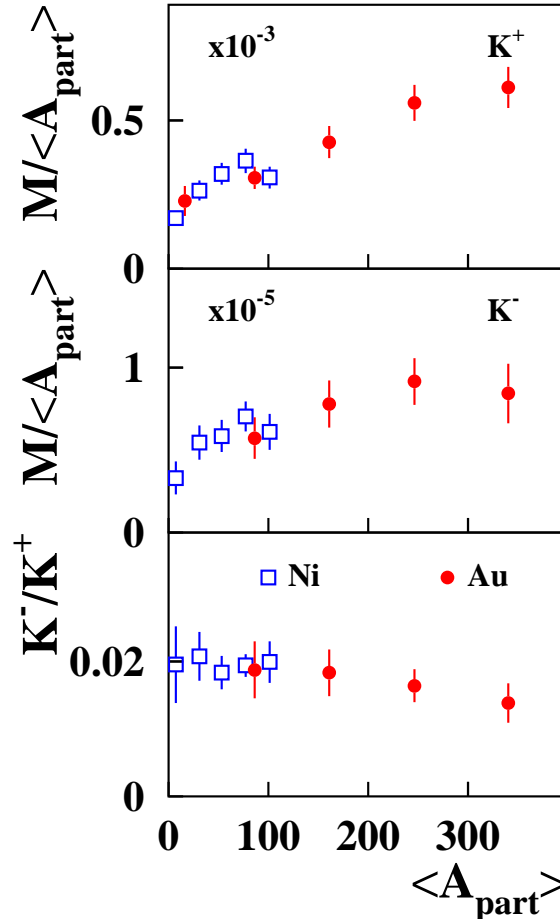


**Figure 5.** Upper panel: The multiplicity of  $K^+$  per number of participating nucleons  $M/\langle A_{part} \rangle$  as a function of  $\langle A_{part} \rangle$  for Au+Au (full circles) and Ni+Ni (open squares) at 1.5 AGeV measured at  $\theta_{lab} = 40^\circ$ . Middle panel: The same but for  $K^-$ . Lower panel: The resulting  $K^-/K^+$  ratio as a function of  $\langle A_{part} \rangle$ .

isotropic distribution this ratio would be constant and identical to 1.

The solid lines in figure 6 represent the function  $1 + a_2 \cdot \cos^2(\theta_{cm})$  which is fitted to the experimental distributions with the values of  $a_2$  given in the figure. In near-central collisions the  $K^-$ -mesons exhibit an isotropic emission pattern whereas the emission of  $K^+$ -mesons is forward-backward peaked. The angular distributions observed for  $K^+$  and for  $K^-$  in Ni+Ni collisions at 1.93 AGeV are similar to the ones presented in figure 6 [11]. The measured emission patterns indicate that the  $K^-$  - in contrast to the  $K^+$  - have lost the memory of the beam direction for central heavy-ion collisions.

#### 4. The time dependence of the $K^+$ - and of the $K^-$ -emission

When summarizing the experimental results on the production and on the propagation of  $K$ -mesons at 1.5 AGeV remarkable similarities and differences between  $K^+$  and  $K^-$

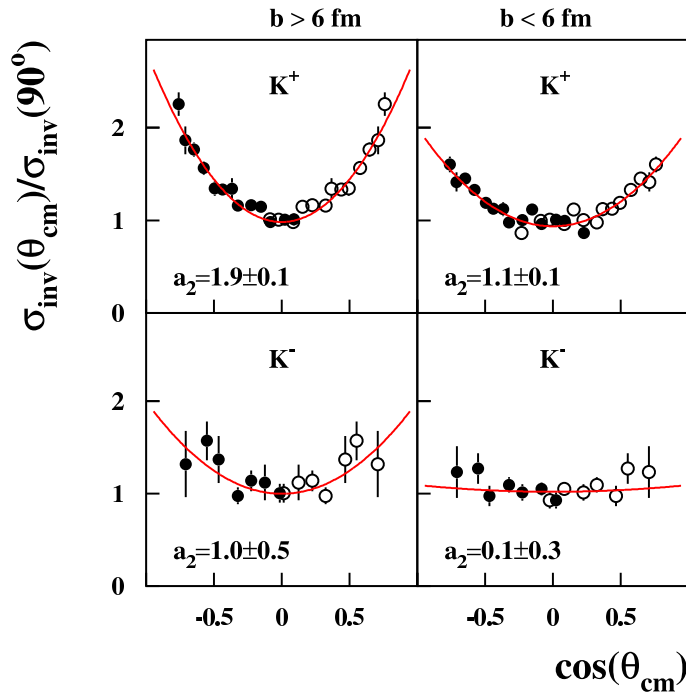


**Figure 6.** Polar angle distributions for  $K^+$  (upper panels) and for  $K^-$  (lower panels) in Au+Au collisions at  $E_{beam} = 1.5$  AGeV. The left panels show data for impact parameters  $b > 6$  fm, the right ones for  $b < 6$  fm. Fits and the parameter  $a_2$  are as described in the text.

are found. The yields of the  $K^+$ - and of the  $K^-$ -mesons are related to each other (as indicated by the almost constant  $K^-/K^+$  ratio as a function of  $\langle A_{part} \rangle$ ). On the other hand, the phase-space distributions (polar angles and spectral slopes) of the  $K^+$ - and of the  $K^-$ -mesons differ significantly. These observations can be explained by the following scenario. In the early phase of the collision the  $K^+$ -mesons and the hyperons are produced via processes like  $NN \rightarrow K^+YN$  or  $\pi N \rightarrow K^+Y$  with  $Y = \Lambda, \Sigma$  [4, 15, 17]. The  $K^+$ -mesons leave the reaction volume with little rescattering because of their long mean free path. Therefore, they probe the early, dense and hot phase of the collision and have been used to obtain information on the nuclear equation-of-state as discussed in section 2. The  $K^-$ -mesons, however, can hardly be produced in direct NN collisions at a beam energy of 1.5 AGeV, even when taking into account Fermi motion. Indeed, transport model calculations predict that in heavy-ion collisions at SIS energies the production and absorption of  $K^-$  predominantly proceeds via strangeness-exchange reactions  $\pi Y \rightleftharpoons K^-N$  [18, 17, 19]. As the  $K^+$  are produced associated with the hyperons the yields of  $K^+$  and  $K^-$  are correlated. Indeed, the measured  $K^-/K^+$  ratio only slightly decreases with increasing centrality, i.e. with the system size.

The mean free path of the  $K^-$ -mesons is about 0.8 fm in nuclear matter due to strangeness-exchange reactions like  $K^-N \rightarrow Y\pi$ . However, via the inverse reaction ( $\pi Y \rightarrow K^-N$ ) the  $K^-$  may reappear again thus propagating to the surface of the reaction volume. Those of the  $K^-$ -mesons which reach the detector are emitted in a late stage of



the collision when the reaction volume is expanding and cooling down. Consequently, the spectral slope of the  $K^-$  is steeper than the one of the  $K^+$ . Furthermore, the emission pattern of the  $K^-$ -mesons is nearly isotropic due to multiple collisions. Both features are observed in the experiment.

The assumption of different emission times for  $K^+$ - and for  $K^-$ -mesons is supported by a transport model calculation using the IQMD code. Figure 7 shows the results of a simulation of central Au+Au collisions ( $b = 0$  fm) at 1.5 AGeV [20]. In the upper panel the time dependence of the density in the reaction zone is given. The lower panel shows the rate  $dN/dt$  of emitted  $K^+$  (solid line) and of emitted  $K^-$  (dashed line) as a function of their production time  $t$ . Within this calculation the  $K^-$  are emitted at a later stage of the reaction during the expansion of the reaction volume while the  $K^+$  are emitted during the high-density phase of the collision.

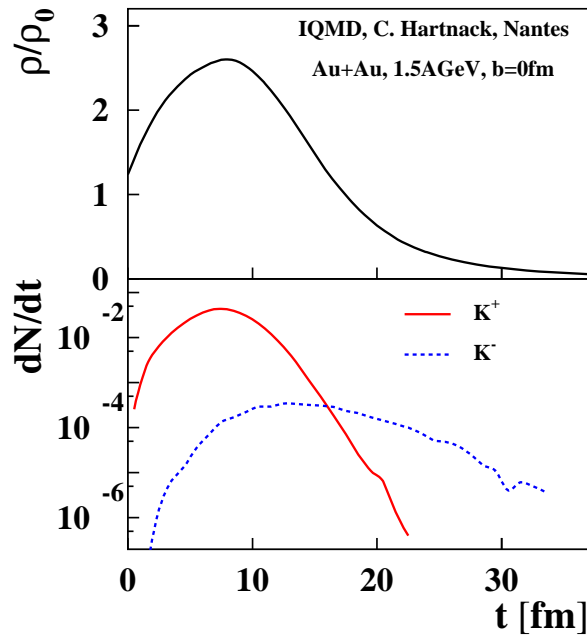


**Figure 7.** The results of an IQMD transport model calculation on the time evolution of a central Au+Au collision [20]. Upper panel: Baryon density  $\rho/\rho_0$  as a function of the time  $t$ . Lower panel: Number of emitted  $K^+$  (solid line) and  $K^-$  (dashed line) per time  $dN/dt$  as a function of their production time  $t$ .

In summary, we have presented differential cross sections and phase-space distributions of  $K^+$ - and of  $K^-$ -mesons produced in heavy-ion collisions at 1.5 AGeV. We observed the following features: (i) The  $K^-/K^+$  ratio is quite independent of  $\langle A_{part} \rangle$  both for Ni+Ni and for Au+Au collisions, (ii) in near-central collisions  $K^-$ -mesons are emitted almost isotropically whereas  $K^+$ -mesons exhibit a forward-backward enhanced emission pattern, and (iii) the inverse slope parameters are significantly smaller for  $K^-$ - than for  $K^+$ -mesons even for the most central Au+Au collisions. These findings indicate that (i) the production mechanisms of  $K^+$ - and of  $K^-$ -mesons are correlated by

strangeness-exchange reactions, (ii) K<sup>-</sup>-mesons undergo many collisions before leaving the reaction volume and, as a consequence, (iii) K<sup>-</sup>-mesons freeze out later than K<sup>+</sup>-mesons.

## References

- [1] J. Aichelin and C. M. Ko, Phys. Rev. Lett. **55** (1985) 2661.
- [2] G. Q. Li, C. H. Lee and G. E. Brown, Phys. Rev. Lett. **79** (1997) 5214.
- [3] C. Sturm et al., Phys. Rev. Lett. **86** (2001) 39.
- [4] C. Fuchs et al., Phys. Rev. Lett. **86** (2001) 1974.
- [5] P. Senger et al., Nucl. Instr. Meth. **A 327** (1993) 393.
- [6] D. Miśkowiec et al., Phys. Rev. Lett. **72** (1994) 3650.
- [7] W. Ahner et al., Phys. Lett. **B 393** (1997) 31.
- [8] R. Barth et al., Phys. Rev. Lett. **78** (1997) 4007.
- [9] Y. Shin et al., Phys. Rev. Lett. **81** (1998) 1576.
- [10] F. Laue, C. Sturm et al., Phys. Rev. Lett. **82** (1999) 1640.
- [11] M. Menzel et al., Phys. Lett. **B495** (2000) 26.
- [12] A. Förster, F. Uhlig et al., accepted for publication by Phys. Rev. Lett. (nucl-ex/0307017).
- [13] G.Q. Li, C.M. Ko, Phys. Rev. **C 54** (1996) R2159.
- [14] J. Schaffner-Bielich, J. Bondorf, I. N. Mishustin, Nucl. Phys. **A 625** (1997) 325.
- [15] J. Aichelin, Phys. Rep. **202** (1991) 233.
- [16] C. Hartnack and J. Aichelin, J. Phys. G **28** (2002) 1649.
- [17] W. Cassing and E. L. Bratkovskaya, Phys. Rep. **308** (1999) 65.
- [18] C.M. Ko, Phys. Lett. **B 138** (1984) 361.
- [19] C. Hartnack, H. Oeschler and J. Aichelin, Phys. Rev. Lett. **90** (2003) 102302.
- [20] C. Hartnack private communication (see also the contribution of C. Hartnack).